Robust constraints on past CO_2 climate forcing from the boron isotope proxy

Hain, M.P.[1]*, Foster, G.L. [2], Chalk, T. [2]

[1] UC Santa Cruz, Earth and Planetary Science, Santa Cruz CA 95064, USA

[2] University of Southampton, Ocean and Earth Sciences, SO143ZH Southampton, UK

* Correspondence to: mhain@ucsc.edu

The atmospheric concentration of the greenhouse gas carbon dioxide, CO_2, is intimately coupled to the carbon chemistry of seawater, such that the radiative climate forcing from CO_2 can be changed by an array of physical, geochemical and biological ocean processes. For instance, biological carbon sequestration, seawater cooling and net $CaCO_3$ dissolution are commonly invoked as the primary drivers of CO_2 change that amplify the orbitally-paced ice age cycles of the late Pleistocene. Based on first-principle arguments with regard to ocean chemistry we demonstrate that seawater pH change (ΔpH) is the dominant control that effectively sets CO_2 radiative forcing (ΔF) on orbital timescales, as is evident from independent late Pleistocene reconstructions of pH and CO_2. In short, all processes relevant for CO_2 on orbital timescales, including temperature change, cause pH to change to bring about fractional CO_2 change so as to yield a linear relationship of ΔpH to CO_2 climate forcing. Further, we show that ΔpH and CO_2 climate forcing can be reconstructed using the boron isotope pH-proxy more accurately than absolute pH or CO_2, even if seawater boron isotope composition is poorly constrained and without information on a second carbonate system parameter. Thus, our formalism relaxes otherwise necessary assumptions to allow the accurate determination of orbital timescale CO_2 radiative forcing from boron isotope-pH reconstructions alone, thereby eliminating a major limitation of current methods to estimate our planet's climate sensitivity from the geologic record.

Key points: **(1)** Radiative forcing by CO_2 linearly related to pH change, second carbonate system parameter not required; **(2)** Using the boron isotope proxy, uncertainty of seawater boron isotopic composition has weaker effect on pH change than absolute pH; **(3)** Short time slices of high-resolution boron isotope data better suited to reconstruct climate forcing than long-term, low-resolution records

1. Introduction

Atmospheric carbon dioxide (CO_2) is a greenhouse gas that causes a radiative forcing of $+3.7 Wm^{-2}$ per CO_2 doubling (e.g., Myhre et al., 1998; Byrne and Goldblatt, 2014) and changes in CO_2 have been identified as important drivers of climate change in the geologic past (e.g., Zachos et al., 2008; Sigman et al., 2010; Shakun et al., 2012). Reconstructing CO_2 change and its associated climate forcing from the geologic record is important for our understanding of the history of physical, chemical and biological changes in the Earth system. In particular, reconstructing the relationships between CO_2 climate forcing and climatic parameters such as temperature, ice sheet mass and sea level provides valuable insights into the couplings and feedbacks operating within Earth's climate system and their dependence on the background climate state (e.g., Martinez-Boti et al., 2015; Chalk et al., 2017). In the context of ongoing warming dominated by anthropogenic carbon emissions Earth's climate sensitivity, the average temperature change per CO_2 doubling, has become a contested parameter of central importance (IPCC, 2014). Given reconstructions of CO_2 and global temperature change it is possible to estimate climate sensitivity from the geologic record (e.g., PALEOSENS Project Members, 2012; Rohling et al., 2017), offering an important test for estimates based purely on computational climate models (e.g., Andrews et al., 2012) and helping to refine estimates of today's climate sensitivity (e.g., Knutti et al., 2017; Goodwin et al., 2018). This is particularly true for past climate intervals that are warmer than the present, implicitly integrating all known and unknown climate feedbacks operating in the Earth system. However, other than for the last 800 thousand years when ice core records accurately capture CO_2 change and its climate forcing, most methods used to reconstruct CO_2 in the more distant and typically warmer-than-present geological past are indirect and generally associated with substantial stochastic and systematic uncertainties (e.g., Royer, 2006; Hemming and Hönisch, 2007; Breecker et al., 2010; Pagani, 2014; Franks et al., 2014; Foster and Rae, 2016). These systematic uncertainties in reconstructing atmospheric CO_2 need to be overcome if we hope to robustly constrain the mechanisms of climate change in general and climate sensitivity in particular from the geologic record.

It is well established that pH and CO_2 are closely tied by seawater carbonate chemistry (Figure 1), with closely aligned contours of constant pH and CO_2. We note further that the spacing of contours of constant pH and $\log_{10}CO_2$ is very similar, which suggests a near linear relationship between H^+ and CO_2. In this study we formally examine this relationship in the context of the boron isotope pH proxy. Our main point is to greatly relax assumptions that are currently required in the reconstruction of CO_2 radiative forcing based on the boron isotope pH proxy, thereby also eliminating a significant source of unnecessary uncertainty and facilitating the exploration of climate sensitivity throughout at least the last 65 million years.

This manuscript is organized as follows. First, in section 2, we lay out the theory that underpins our formalism of the relationship between pH change (ΔpH) and CO_2 radiative forcing (ΔF). Then we use mathematical derivations and numerical solutions to demonstrate the reason why ΔpH and ΔF change in unison regardless of whether these changes are caused by the addition/removal of carbon and $CaCO_3$ or increases/decreases in temperature. Second, in section 3, we show that the observed relationship of ΔpH change and independently reconstructed ΔF from ice core measurements of the last 260 thousand years indeed agrees with our theory, that ΔpH can be robustly reconstructed using the boron isotope pH proxy even if the boron isotopic composition of seawater is poorly constrained, and that applying our formalism can yield useful constraints on climate sensitivity. Finally, in section 4, we critically assess the caveats and assumptions of our formalism, discussing specifically when our approach should not be applied and considerations for the sampling strategy best suited to constrain ΔF and climate sensitivity from the geologic record. Overall, our study suggests that it is possible to use the boron isotope pH proxy to derive robust estimates of past ΔpH, ΔF and climate sensitivity even if (a) the cause of past CO_2 change is unknown, (b) the boron isotopic composition of seawater is poorly constrained, and (c) without information on a second carbonate system parameter.

2. Formalism and derivations

If the goal is to estimate absolute CO_2 concentrations based on reconstructed pH then there are no shortcuts to the established formalism (e.g., Zeebe and Wolf-Gladrow, 2001), which requires e.g. accurate measurement of boron isotopic composition of planktonic foraminifera, correction for vital effects, temperature and salinity reconstructions, accurate knowledge of seawater boron isotopic composition, equilibrium constant corrections for seawater major ion change, and a fully independent estimate of a second carbon chemistry parameter. The latter point especially is a major problem because no method currently exists to reconstruct seawater carbon concentration or alkalinity and their changes over geologic time. However, to calculate CO_2 climate forcing (ΔF, in Wm^{-2}) we do not need to know absolute CO_2, or even absolute CO_2 change, but only fractional CO_2 change (i.e., the change in the logarithm of CO_2, $\Delta \log CO_2$):

$$\Delta F = \alpha_{2xCO2} * \Delta \log_2 CO_2 = \frac{\alpha_{2xCO2}}{\log_{10} 2} * \Delta \log_{10} CO_2 \quad \text{(eq. 1)}$$

where α_{2xCO2} is the sensitivity of the radiative balance per CO_2-doubling, $\Delta \log_2 CO_2$. For large parts of the subtropical and tropical ocean the carbon and acid/base chemistry of surface waters remain near equilibrium with atmospheric CO_2 because of shallow mixed layer depth and strong density stratification that greatly restricts exchange between equilibrating surface water and underlying waters (Takahashi et al., 2002, 2009; Rödenbeck et al., 2013). Assuming that surface water CO_2 partial pressure in these regions tracks atmospheric CO_2 the fractional CO_2 change relative to a reference, $\Delta \log_{10} CO_2 = [\log_{10} CO_2] - [\log_{10} CO_2]_{reference}$, can be expressed as follows:

$$CO_2 + H_2O \overset{K_0, K_1}{\Longleftrightarrow} H^+ + HCO_3^- \quad \text{(eq. 2a)}$$

$$CO_2 = \frac{H^+ * HCO_3^-}{K_0 * K_1} \quad \text{(eq. 2b)}$$

$$\log_{10} CO_2 = \log_{10} HCO_3^- + pK_0 + pK_1 - pH \quad \text{(eq. 2c)}$$

$$\Delta \log_{10} CO_2 = \Delta \log_{10} HCO_3^- + \Delta pK_0 + \Delta pK_1 - \Delta pH \approx -\Delta pH \quad \text{(eq. 2d)}$$

Equation 2a is the chemical equation for the equilibrium of reversible CO_2 hydration and deprotonation to bicarbonate and free proton, and Equation 2b quantitatively describes this standard relationship between CO_2 and seawater carbonate chemistry. To yield a distinct pH term in Equation 2c we take the logarithm of equation 2b. To write Equation 2d as an expression that relates fractional CO_2 change ($\Delta\log_{10}CO_2$) to pH change (ΔpH) we take the difference between two states of carbonate chemistry written in the form of Equation 2c. The other terms appearing in Equation 2 are the bicarbonate concentration HCO_3^-, and the carbonate chemistry equilibrium constants K_0 and K_1. Bicarbonate is by far the dominant form of carbon and therefore approximates the total dissolved inorganic carbon (DIC) concentration. The carbonate system equilibrium constants change with temperature, salinity and seawater major ion composition.

The basic argument of this study is that the right-hand side of equation 2d is dominated by ΔpH, and thus past fractional CO_2 change may be usefully constrained by reconstructing pH change alone. If so, combining equations 1 and 2 yields a linear relationship between pH change (ΔpH) and climate forcing from atmospheric CO_2 change (ΔF):

$$\Delta F \approx 3.7 \frac{W}{m^2} * \Delta\log_2 H^+ = -12.3 \frac{W}{m^2} * \Delta pH \qquad \text{(eq. 3)}$$

Our formalism posits that fractional CO_2 change is dominantly caused by pH change, without specifying the set of processes responsible for the pH change and without assessing the magnitude of the error incurred by using that approximation. In the following sections we demonstrate that both carbon and $CaCO_3$ addition/removal (section 2.1) as well as the temperature effects on CO_2 solubility and equilibrium constants (section 2.2) indeed cause very similar fractional change in H^+ and CO_2, thereby yielding a linear relationship between ΔpH and ΔF as posited by our formalism.

2.1 Carbon and $CaCO_3$ addition/removal

The carbon chemistry of seawater is tied to the overall concentration of dissolved inorganic carbon (DIC) and the relative excess of dissolved bases over acids, alkalinity

(ALK). Biological production or respiration of soft-tissue organic matter mainly removes or adds carbon to seawater, with only a very small effect on ALK. Conversely, biological production of $CaCO_3$ and its dissolution act to change ALK and DIC in a strict 2-to-1 ratio. The formalism outlined above presumes that the addition or removal of both DIC and $CaCO_3$ causes most of its effect on CO_2 by changing the partitioning of DIC among carbonic acid, bicarbonate ion and carbonate ion, as reflected by pH change, rather than by changing the total dissolved carbon concentration itself (i.e., little change in the HCO_3^- term in Equation 2). To assess the validity of this assertion we impose DIC and $CaCO_3$ addition/removal and use a carbonate chemistry solver to calculate the resulting changes in pH and CO_2 (Figure 2; see panel a for DIC perturbation and panel b for $CaCO_3$ perturbation). Our formalism posits that the fractional change in H^+ equals the fractional change in CO_2, such that $\Delta\log_{10}CO_2$ equals ΔpH (i.e., solid black line in Figure 2d). When cross-plotting calculated pH and CO_2 (on a logarithmic axis) we find that both DIC and $CaCO_3$ addition/removal result in a linear pH-to-$\log_{10}CO_2$ relationship, but the slope of that relationship is about 30% steeper for DIC and about 10% less steep for $CaCO_3$ addition/removal than posited by our formalism. That is, while our basic formalism presumes an equal magnitude of ΔpH and $\Delta\log_{10}CO_2$ (e.g., equation 2) the consistent deviations from that expectation for DIC and $CaCO_3$ addition/removal span an end-member $\Delta\log_{10}CO_2/\Delta$pH range of about -1.3:1 and -0.9:1 that needs to be propagated when using Equation 3 to infer CO_2 climate forcing from pH change.

To clarify why DIC and $CaCO_3$ addition/removal cause $\Delta\log_{10}CO_2/\Delta$pH that deviates from unity and to demonstrate that these deviations are robust and expected it is useful to consider the formal mathematical expressions of CO_2 change in response to a DIC perturbation (i.e., δ_C) and a $CaCO_3$ perturbation (i.e., δ_{CaCO3}), respectively, at constant temperature and salinity (i.e., no change in the equilibrium constants; see also section 2.2 for changing equilibrium constants in response to temperature change). That is, we wish to derive the partial derivatives of equilibrium CO_2 and equilibrium H^+, which depend on bicarbonate ion (HCO_3^-) and carbonate ion (CO_3^{2-}) concentration:

$$CO_2 = \frac{H^+ * HCO_3^-}{K_0 * K_1} \quad \text{(eq. 4a)}$$

$$H^+ = \frac{K_2 * HCO_3^-}{CO_3^{2-}} \quad \text{(eq. 4b)}$$

In order to write the partial derivatives of CO_2 and H^+ we need to know the bicarbonate and carbonate ion partial derivatives to incremental chemical change, and we use the CPF (carbonate proton fraction) notation of Hain et al. (2015) to keep our expressions concise. CPF equates to the fraction of total seawater buffering that is due to the bicarbonate/carbonate ion buffer (i.e., seawater CPF of about -0.65 means that per unit of acid added carbonate ion is reduced and bicarbonate increased by 0.65 units):

$$\frac{\delta CO_3^{2-}}{\delta C} = CPF \approx \frac{-1}{1+B(OH)_4^-/CO_3^{2-}} \sim -0.65 \quad \text{(eq. 5a)}$$

$$\frac{\delta HCO_3^-}{\delta C} = 1 - CPF \quad \text{(eq. 5b)}$$

$$\frac{\delta CO_3^{2-}}{\delta ALK} = -CPF \quad \text{(eq. 5c)}$$

$$\frac{\delta HCO_3^-}{\delta ALK} = CPF \quad \text{(eq. 5d)}$$

The partial derivatives of H^+ and CO_2 with respect to small perturbations of DIC and ALK (δ_C and δ_{ALK}) are obtained using the quotient and product rule, respectively, and substituting equations 5a-d to take the place of the bicarbonate and carbonate ion partial derivatives:

$$\frac{\delta_C H^+}{\delta C} = \frac{(1-CPF)*K_2}{CO_3^{2-}} - \frac{CPF*K_2*HCO_3^-}{(CO_3^{2-})^2} \quad \text{(eq. 6a)}$$

$$\frac{\delta_{ALK} H^+}{\delta ALK} = \frac{(CPF)*K_2}{CO_3^{2-}} - \frac{-CPF*K_2*HCO_3^-}{(CO_3^{2-})^2} \quad \text{(eq. 6b)}$$

$$\frac{\delta_C CO_2}{\delta C} = \left\{\frac{\delta HCO_3^-}{\delta C} * \frac{H^+}{K_0*K_1}\right\} + \left[\frac{\delta H^+}{\delta C} * \frac{HCO_3^-}{K_0*K_1}\right] = \left(\{1 - CPF\} + \left[1 - CPF - \frac{H^+}{K_2} CPF\right]\right) * \frac{CO_2}{HCO_3^-} \quad \text{(eq. 6c)}$$

$$\frac{\delta_{ALK} CO_2}{\delta ALK} = \left\{\frac{\delta HCO_3^-}{\delta ALK} * \frac{H^+}{K_0*K_1}\right\} + \left[\frac{\delta H^+}{\delta ALK} * \frac{HCO_3^-}{K_0*K_1}\right] = \left(\{CPF\} + \left[CPF + \frac{H^+}{K_2} CPF\right]\right) * \frac{CO_2}{HCO_3^-} \quad \text{(eq. 6d)}$$

The partial derivative of H^+ and CO_2 with respect to small perturbation of $CaCO_3$ (i.e., δ_{CaCO3}) is simply the sum of equations 6a/b and 6c/d weighted by the 2:1 stoichiometric ALK-to-DIC ratio of $CaCO_3$:

$$\frac{\delta_{CaCO_3}H^+}{\delta CaCO_3} = \frac{\delta_C H^+}{\delta C} + 2 * \frac{\delta_{ALK}H^+}{\delta ALK} \quad \text{(eq. 7a)}$$

$$\frac{\delta_{CaCO_3}CO_2}{\delta CaCO_3} = \frac{\delta_C CO_2}{\delta C} + 2 * \frac{\delta_{ALK}CO_2}{\delta ALK} \quad \text{(eq. 7b)}$$

To arrive at the final desired expressions of fractional CO_2 change, we separate the differential and rearrange equations 6c and 7b:

$$\frac{\delta_C CO_2}{CO_2} = \left(\{1 - CPF\} + \left[1 - CPF - \frac{H^+}{K_2} CPF\right]\right) * \frac{\delta C}{HCO_3^-} \quad \text{(eq. 8a)}$$

$$\frac{\delta_{CaCO_3}CO_2}{CO_2} = \left(\{1 + CPF\} + \left[1 + CPF + \frac{H^+}{K_2} CPF\right]\right) * \frac{\delta CaCO_3}{HCO_3^-} \quad \text{(eq. 8b)}$$

Both equations relate left-hand side fractional CO_2 change (i.e., incremental CO_2 change δCO_2 divided by background CO_2) to its underlying carbon chemistry causes due to carbon addition (i.e., eq. 8a: incremental carbon addition δC divided by background bicarbonate ion concentration) and $CaCO_3$ addition (i.e., eq. 8b: incremental $CaCO_3$ addition $\delta CaCO_3$ divided by background bicarbonate ion concentration). The curly brackets on the right-hand side are arranged to highlight the effect of changing bicarbonate concentration whereas the square brackets highlight the effects of changing pH.

Substituting reasonable values for H^+/K_2 and CPF into equations 8a and 8b we find that the pH effect dominates over the effect of bicarbonate abundance, in the case of DIC addition by about 3.4-fold (i.e., a square bracket pH change term of 5.55 relative to the curly bracket term of 1.65 for the effect of bicarbonate abundance, equation 8a) and in the case of $CaCO_3$ addition by 10-fold (i.e., a square bracket pH change term of -3.55 relative to the curly bracket term of 0.35, equation 8b). That is, the relationships between ΔpH and $\Delta\log_{10}CO_2$ are not exactly -1:1 as approximated in equation 2d, but based on equation 8 we estimate -1:1.3 for carbon addition/removal and -1:0.9 for $CaCO_3$ addition/removal (the range between these end-members is shown as gray shading in Figure 2d).

The slightly stronger and weaker than predicted CO_2-to-pH relationships for incremental DIC and $CaCO_3$ addition/removal, respectively, are quantitatively consistent with the carbonate chemistry solver results shown in Figure 2, underscoring on a mechanistic level that pH change caused by DIC and $CaCO_3$ addition/removal is the dominant driver of CO_2 change whereas the much weaker effect of changing bicarbonate abundance is responsible for the deviation of the ΔpH-to-$\Delta\log_{10}CO_2$ relationship from the -1:1 solely pH-driven slope (i.e., solid black line in Figure 2d). Based on these deviations, if pH change is known exactly then $\Delta\log_{10}CO_2$ and CO_2 climate forcing can be estimated to within the end-member bounds of -10% for purely $CaCO_3$-caused and +30% for purely DIC-caused carbon chemistry change (i.e., gray shading in Fig 1d), with any combination of these drivers yielding less bias relative to the formalism of equations 2 and 3. Later in the manuscript, in section 3.3, we will use this theoretically derived end-member uncertainty envelope when estimating CO_2 climate forcing from pH change.

2.2 Temperature change

All of what is said above ignores the strong effects of temperature on the solubility of CO_2 in seawater and on the equilibrium constants that govern the deprotonation equilibria of carbonic acid and bicarbonate ion: i.e., K_0, K_1 and K_2. This raises the question if temperature change associated with CO_2 climate forcing can reduce the utility of our formalism for estimating CO_2 climate forcing from reconstructed pH change. That is, does temperature change CO_2 independently of pH? To address this question we derive the sensitivity of fractional CO_2 change to incremental change in temperature, and we use a carbonate chemistry solver to confirm that temperature change cause fractional CO_2 and H^+ changes very close to the posited -1:1 relationship.

Analogous with the derivation of the DIC and $CaCO_3$ effects above, we use the product rule to arrive at the partial derivative of H^+ and CO_2, but this time due to temperature change in absence of DIC or ALK perturbation. Since the speciation of the set concentration of carbon is constrained by the set ALK we take the partial derivatives of bicarbonate and carbonate ion to be zero (a very good approximation) and only consider

changes in the equilibrium constants and the minor species [H^+] and (implicitly) carbonic acid:

$$\frac{\delta_T H^+}{\delta T} \cong \frac{HCO_3^-}{CO_3^{2-}} * \frac{\delta_T K_2}{\delta T} = \frac{CO_2}{K_2} * \frac{\delta_T K_2}{\delta T} \quad \text{(eq. 9a)}$$

$$\frac{\delta_T CO_2}{\delta T} \cong \left\{\frac{-CO_2}{K_0 * K_1} * \frac{\delta_T (K_0 * K_1)}{\delta T}\right\} + \left[\frac{CO_2}{K_2} * \frac{\delta_T K_2}{\delta T}\right] \quad \text{(eq. 9b)}$$

To arrive at the final desired expression of fractional CO_2 change in response to temperature change we separate the differential and rearrange equation 9b:

$$\frac{\delta_T CO_2}{CO_2} \cong \left\{-\frac{\delta_T K_0}{K_0} - \frac{\delta_T K_1}{K_1}\right\} + \left[\frac{\delta_T K_2}{K_2}\right] \approx \left(\left\{\frac{3\%}{^\circ C} - \frac{2.5\%}{^\circ C}\right\} + \left[\frac{3.5\%}{^\circ C}\right]\right) * \delta T \quad \text{(eq. 10)}$$

From this approximation we find three dominant terms governing CO_2 sensitivity to incremental warming that can be described as: (K_0 term) a fractional decrease in CO_2 solubility K_0 causes a fractional CO_2 increase; (K_1 term) at a given pH a fractional increase in the bicarbonate-to-carbonic acid equilibrium constant K_1 causes a fractional CO_2 decrease; and (K_2 term) constant DIC and ALK demand that the carbonate-to-bicarbonate ion ratio is nearly constant so that a fractional increase in the carbonate-to-bicarbonate ion equilibrium constant K_2 causes a fractional increase of H^+. This latter fractional H^+ increase, a pH decline, translates to a fractional increase in CO_2. Put a different way, the K_0 and K_1 effects (curly bracket in equation 10) operate mainly by changing the abundance and solubility of the least abundant dissolved inorganic carbon species, carbonic acid, whereas the K_2 effect (square bracket) changes the pH at which the main seawater acid/base buffer, bicarbonate-to-carbonate ion, is at equilibrium.

When using a carbonate chemistry solver we find the net sensitivity of CO_2 to temperature change (at constant DIC and ALK) is about a 4% increase per degree of warming (Figure 2c), which agrees very well with the sum of the three individual effects isolated in equation 10. Likewise, the carbonate chemistry solver yields about 3.5% H^+ increase per degree of warming, fully consistent with the square bracket K_2 term in equation 10. All three terms in equation 10 have a similar magnitude, but the two terms (K_0, K_1) that operate through carbonic acid have opposite sign and nearly cancel each

300 other whereas the K_2 term that operates through pH is unopposed. For this reason, the pH-driven CO_2 change (square bracket) is 7-fold greater than the CO_2 change driven by
302 the combination of carbonic acid solubility and deprotonation (curly bracket; equation 10). Thus, by fortuitous coincidence, the sensitivities of fractional H^+ change and
304 fractional CO_2 change to incremental warming or cooling is approximately the same (Figure 2c), yielding a -1:1.14 ΔpH-to-$\Delta\log_{10}CO_2$ relationship that is close to the -1:1
306 approximation in equation 2d, and it falls within the end-member range of DIC and $CaCO_3$ addition/removal (see section 2.1). That is to say, the net effect of temperature on
308 fractional CO_2 change can be estimated from pH change in the very same way as CO_2 change caused by the addition or removal of DIC and $CaCO_3$ (Figure 2c and 2d).
310

3 Validation and Applications

312 3.1 Relationship of pH and ice core CO_2

Our formalism, equation 3, suggests that on orbital timescales there should be a linear
314 relationship between CO_2 radiative climate forcing and pH change of the well-equilibrated subtropical ocean surface, with the slope of that relationship effectively set
316 by the independently determined (e.g., Myhre et al., 1998; Byrne and Goldblatt, 2014) radiative effect per CO_2 doubling. We test this assertion by combining the continuous late
318 Pleistocene ice core atmospheric CO_2 record with overlapping boron isotope measurements on planktonic foraminifera. Recently collected data from ODP Site 999
320 (Chalk et al., 2017) offers the unique opportunity to rigorously test the theory over the last 260 thousand years.
322

Ice core CO_2 data are precise, accurate (e.g., Bereiter et al., 2015) and using equation 1
324 can be easily converted into climate forcing, ΔF. Foraminiferal boron isotope data can be used to reconstruct surface pH given auxiliary knowledge of temperature and bulk
326 seawater boron isotopic composition (Vengosh et al., 1991; Hemming and Hanson, 1992; Spivack et al., 1993; Zeebe and Wolf-Gladrow, 2001; Foster and Rae, 2016). For the
328 purpose of this proof-of-concept test we use Mg/Ca-based SST data only to account for the temperature effect on the pH reconstruction (i.e., pK_B temperature dependence; using
330 our formalism we need not calculate the carbonate chemistry equilibrium constants pK_0,

pK_1 and pK_2) and we presume known modern boron isotopic composition of seawater (39.61 ‰; Foster et al., 2010), as is appropriate for the late Pleistocene given the multi-million year ocean residence time of boron (Spivack and Edmont, 1987; Lemarchand et al., 2002). The new boron isotope and Mg/Ca data (Chalk et al., 2017) that overlaps with the ice core CO_2 record was measured at the University of Southampton using established and extensively documented methods (Foster, 2008; Foster et al., 2013). The 1σ age uncertainty of the data is 1 kyrs and 1.5 kyrs for the for data points younger and older than 10 kyrs, respectively.

To account for the significant age uncertainty of the boron isotope data when compared to the well-dated ice core data we calculate the cumulative probability density of the ice core data within the ±4σ age uncertainty interval, normalized by their respective likelihood given the age difference. This approach yields small uncertainty in CO_2-driven ΔF at times that coincide with intervals of the ice core record with relatively constant CO_2, and it yields large ΔF uncertainty for ages corresponding to rapid CO_2 change. That is, while the ice core CO_2 data itself is very accurate and well-dated the age uncertainty of the boron isotope data implies significant uncertainty in $\Delta F_{ice\text{-}core}$ at the time of the $\delta^{11}B$-based reconstruction of pH. Plotting $\Delta F_{ice\text{-}core}$ as a function of the corresponding reconstructed pH yields a strong apparent negative correlation (Figure 3). We also plot the 1σ uncertainty intervals corresponding to the internal reproducibility of the underlying boron isotope measurement (horizontal error bars) as well as the 1σ of $\Delta F_{ice\text{-}core}$ corresponding to the age uncertainty the sediment samples (vertical error bars), which together can explain most of data scatter.

To determine the best-fitting linear model we use York regression (York et al., 2004), which accounts for uncertainty in both x and y. The dark and light blue shading in Figure 3 represents the 1σ and 2σ envelope of the maximum likelihood model (i.e., $\Delta F/\Delta pH = -13.3$ W/m^2; with 1σ of 0.5 W/m^2). That is, the best-fitting model through the data is very close to the theoretical $\Delta F/\Delta pH$ relationship of -12.3 W/m^2 (solid black line in Figure 3) and indeed we cannot reject the null hypothesis that the data results from a strict adherence to our basic formalism (i.e., equation 3) plus random Gaussian error. This error

362 term can be estimated from the residuals to be 1σ of ~0.32W/m^2 and it corresponds to the superposition of boron isotope measurement uncertainty, age error, air/sea
364 disequilibrium, etc.

366 In the above analysis we have validated our basic formalism without considering that equation 3 is a useful approximation rather than a first-principle law. As is evident from
368 Figure 2d and equations 8 and 10 the first principle slope of the ΔF/ΔpH relationship is ~14-30% steeper if the driving process is a change in temperature or DIC
370 addition/removal, while it is ~10% less steep when caused by $CaCO_3$ addition/removal. In this context, we can reject the null hypothesis that overall glacial-interglacial CO_2
372 change and its climate forcing were exclusively driven by either biological sequestration of carbon or ocean alkalinity changes via the open system $CaCO_3$ cycle. This outcome is
374 consistent with the large body of evidence that glacial cooling, carbon sequestration from the atmosphere and upper ocean via the biological pump into the deep ocean, as well as
376 whole ocean alkalinity increase related to transient and steady state lysocline change all contributed to ice age CO_2 drawdown (e.g., Sigman and Boyle, 2000; Martinez-Garcia,
378 2014; Sigman et al., 2010; Hain et al., 2014; Wang et al., 2017). Because the best-fitting regressed slope falls between the $CaCO_3$ end-member on one side and the temperature
380 and DIC end-members on the other side we conclude that a relatively large portion of overall glacial/interglacial CO_2 change appears to have been driven by changes in whole
382 ocean alkalinity related to transient imbalances in the ocean's open system $CaCO_3$ cycle, resonating with one of the earliest hypothesis to explain these changes (Broecker and
384 Peng, 1987). All of these processes have acted at different times in the glacial progression (e.g., Hain et al. 2010), such that their relative contribution to CO_2 drawdown and the
386 effective relationship between CO_2 and pH evolved with time. In this context, it seems plausible to decompose the relative contribution of DIC, alkalinity and temperature
388 changes to overall glacial/interglacial CO_2 change based on the regression of ΔF/ΔpH, but such analysis would require additional global carbon cycle modeling that is beyond
390 the scope of this study. For the purpose of this work we note that the empirical ΔpH/ΔF slope falls well within the end member ΔpH/ΔF range for DIC and $CaCO_3$ changes, and
392 that this range can be used to represent the uncertainty in the conversion from ΔpH to ΔF.

394 **4.2 Seawater boron isotope composition**

The approach described above only requires a record of past pH changes to reconstruct
396 CO_2 climate forcing, thereby making independent knowledge of background ocean carbon concentration (DIC) and temperature for the purpose of calculating the carbon
398 chemistry equilibrium constants K_0, K_1 and K_2, unnecessary. However, to reconstruct pH from boron isotope data (i.e., $\delta^{11}B_{borate}$) still requires independent constraints on the bulk
400 boron isotopic composition of seawater ($\delta^{11}B_{SW}$) as well as temperature and salinity for the purpose of calculating the borate/boric acid equilibrium constant pK_B (e.g., Zeebe and
402 Wolf-Gladrow, 2001), which is weakly dependent also on seawater major ion composition (Hain et al, 2015) and may thus require minor correction for the deep
404 geologic past (Henehan et al., 2016). This raises the question: Can we use boron isotope data to reconstruct CO_2 climate forcing in deep geologic time, when bulk seawater boron
406 isotopic composition is poorly constrained and temperature reconstructions are questionable at least in their absolute sense? Or, put a different way, is the boron isotope
408 pH proxy inherently more robust in reconstructing past pH *change* than in reconstructing *absolute* pH? To answer these questions we first consider the established boron isotope
410 pH proxy equation for a single sample (Zeebe and Wolf-Gladrow, 2001):

412 $$pH_0 = pK_B - \log_{10}\left(\frac{\delta_0 - \delta_{SW}}{\delta_{SW} - \alpha * \delta_0 - \epsilon}\right) \quad \text{(eq. 11)}$$

414 where ε and α are the equilibrium boron isotope effect and fractionation factor (i.e., 27.2‰ and 1.0272; see Klochko et al., 2006), δ_{SW} is the boron isotopic composition of
416 bulk seawater, δ_0 is the reconstructed boron isotopic composition of borate from which pH is to be calculated, and pK_B is the borate/boric acid equilibrium constant when δ_0 was
418 formed. Accurate reconstruction of absolute pH using this formulation requires accurate reconstruction of both δ_0 and δ_{SW}, and accurate auxiliary information on absolute
420 temperature, salinity and seawater major ion composition to calculate pK_B. Notably, δ_0 and δ_{SW} carry equivalent weight in the established boron isotope pH proxy equation but
422 for much of Earth history δ_{SW} is much more uncertain than reconstructions of δ_0.

To contrast the established formulation we write the proxy equation for pH change (ΔpH) reconstructed from a set of two borate boron isotope reconstructions, δ_0 and δ_1:

$$\Delta pH = pH_1 - pH_0 = \Delta pK_B - \log_{10}\left(\frac{\delta_1 - \delta^{11}B_{SW}}{\delta_{SW} - \alpha * \delta_1 - \epsilon} * \frac{\delta_{SW} - \alpha * \delta_0 - \epsilon}{\delta_0 - \delta_{SW}}\right)$$

$$= \Delta pK_B - \log_{10}\left(1 + \frac{\delta_1 - \delta_0}{\delta_{SW} - \alpha * \delta_1 - \epsilon} * \frac{(\alpha - 1) * \delta_{SW} - \epsilon}{\delta_0 - \delta_{SW}}\right) \quad \text{(eq. 12)}$$

While δ_{SW} is still required to calculate ΔpH the dominant boron isotope term in the ΔpH equation is the difference between δ_1 and δ_0, which has two very significant implications. First, any error in δ_{SW} causes greater error in reconstructed pH than in ΔpH, such that ΔpH can be more accurately reconstructed than absolute pH in the face of δ_{SW} uncertainty. Second, the reconstructed values of δ_0 and δ_1 need to be precise but not necessarily accurate as long as they carry the same systematic bias (e.g., from vital effects, matrix differences between the sample material and the measurement standard, etc.), which makes the reconstruction of ΔpH inherently more robust than the reconstruction of absolute pH. Additionally, ΔpK_B only weakly depends on only relative changes in temperature, salinity and seawater major ion composition, not absolute values, such that ΔpK_B is smaller and can be more accurately reconstructed than pK_B. Overall, our examination of the pH and ΔpH proxy equations demonstrates that reconstructions of ΔpH are both more accurate in the face of δ_{SW} uncertainty and more robust in the face of a number of potential biases than is the reconstruction of absolute pH. We anticipate that this finding will not come as a major surprise to practitioners in the field of boron isotope geochemistry, but to our knowledge this is the first formal statement of the fact.

Based on the above theoretical considerations we should be able to recover the correct relationship between CO_2 climate forcing (ΔF) and pH change (ΔpH) even if we were to completely ignore temperature change (e.g., because ΔpK_B is only a relatively weak function of temperature change) and even if we were to deliberately introduce significant error in the bulk seawater boron isotopic composition (e.g., because δ_{SW} has little weight on the value of the logarithmic term in equation 12). To demonstrate the pervasive differences in the reconstruction of pH and ΔpH we turn again to the comparison of the

boron isotope measurements from ODP Site 999 and the coeval ice core record of
454 atmospheric CO_2 (as in Figure 3) but this time systematically changing the bulk seawater boron isotopic composition ($\delta^{11}B_{SW}$, same as abbreviated δ_{SW} notation in equations 11
456 and 12) used in the calculation by ±4.2‰ around its true value of 39.61‰ (Figure 4). Also, we find no noticeable difference when including or excluding the effect of
458 reconstructed local temperature changes on pK_B, and for the purpose of highlighting the role of δ_{SW} uncertainty we show the results where pK_B is taken to be constant.
460

As expected the very large range of deliberately introduced offset in seawater boron
462 isotopic composition systematically increases/decreases the mean absolute pH by more than 0.07 pH units per 1‰ of $\delta^{11}B_{SW}$ change (Figure 4a). That is, absolute pH is highly
464 sensitive to the assumed $\delta^{11}B_{SW}$ (see also Pagani et al., 2005). In stark contrast, however, the pH range covered by the ODP Site 999 dataset changes much less as $\delta^{11}B_{SW}$ is
466 manipulated, such that the regressed $\Delta F/\Delta pH$ slope changes only mildly even in the face of substantial introduced $\delta^{11}B_{SW}$ error. Specifically, comparison of the regressed slope
468 (blue envelope) to the relationship theoretically predicted by equation 3 suggests that the theory is a reasonably good predictor for the true ice core-derived ΔF even in the face of
470 $\delta^{11}B_{SW}$ error as large as ±2‰ (x-axis in Figure 4b), which compares favorably with the uncertainty of $\delta^{11}B_{SW}$ reported in available reconstructions (e.g., Lemarchand et al., 2000;
472 Raitzsch and Hönisch, 2013; Greenop et al., 2017).

474 We note that we calculate the results shown in Figure 4 using the established pH proxy equation, and that our formulation of ΔpH (i.e., equation 12) simply expresses the
476 difference between two standard pH reconstructions. The main point we intend to demonstrate in this section is that $\delta^{11}B_{SW}$ uncertainty affects pH significantly more than it
478 does ΔpH, both reconstructed using the same established boron isotope proxy equation. That is, the boron isotope proxy system inherently yields more robust estimates of past
480 pH change than absolute pH. Earlier we showed in theory (see section 2) and observations (see section 3.1) that pH change (ΔpH) is a strong predictor for CO_2 climate

482 forcing. In that context, our ability to obtain robust reconstructions of ΔpH from the boron isotope proxy is critical.

484

3.5 Climate sensitivity

486 Reconstructing CO_2 radiative forcing using the boron isotope pH proxy offers important insights into the role of the global carbon cycle in causing climate change of the geologic 488 past. However, in the context of ongoing anthropogenic climate change and when comparing different periods of geologic time the quantity of interest is often the climate 490 sensitivity S, which is the ratio of temperature change (ΔT) per radiative climate forcing (ΔF) (e.g., Knutti and Hegerl, 2008):

492

$$S = {}^{\Delta T}/_{\Delta F} \qquad \text{(eq. 13)}$$

494

In the case that only the component of total forcing that is due to CO_2 is explicitly 496 considered the climate sensitivity calculated in this way is commonly referred to as Earth System Sensitivity (ESS; Lunt et al. 2010), which implicitly includes climate system 498 feedbacks that are 'fast' (e.g., water vapor, clouds) and 'slow' (e.g., dust, ice sheets). Also, there exists a spectrum of alternate definitions of climate sensitivity that explicitly 500 include the component climate forcing of a number of these "slow" processes (e.g., PALEOSENS, 2012; von der Heydt et al., 2016). We note that all formulations of climate 502 sensitivity require constraints on CO_2 climate forcing, which is the focus of our study, but detailed treatment of different types and ways to calculate climate sensitivity is beyond 504 our scope here. That said, given the uncertainties of boron isotope measurements and the range in the ΔpH-to-ΔF conversion for different end-member causes of pH change (i.e., 506 $CaCO_3$, temperature and DIC change as described above, Figure 2), we need to address the question if our formalism can yield sufficiently accurate and precise constraints on 508 ΔT/ΔF. To address this question we need a target estimate of "true" ΔT/ΔF and compare it to the equivalent result based on boron isotope data. For this test we again turn to the 510 ice core CO_2 record (as compiled by Bereiter et al., 2015) to yield "true" CO_2 radiative forcing, which we pair with two independent reconstructions of temperature change over 512 the late Pleistocene glacial/interglacial cycles (global mean surface air temperature MAT

and sea surface temperature SST taken from Martinez-Boti et al., 2015). We note that SST does not reflect global mean surface temperature such that using this record is not intended to yield bona fide estimates of climate sensitivity but to evaluate the accuracy and precision of our formalism in constraining climate sensitivity. Conversely, MAT is based on inverse model results of northern hemisphere temperature (i.e., van de Wal et al., 2011) scaled to reflect global mean surface temperature for the purpose of calculating climate sensitivity (see Martinez-Boti et al., 2015).

We interpolate the temperature records at the ages of the 1011 discrete ice core CO_2 data points of the last 260 kyrs and determine $\Delta T/\Delta F$ by regressing the slope of temperature change per ice core CO_2-derived climate forcing using the York regression method (York et al., 2004), assuming 1σ uncertainty of 1˚C and 5 ppmV for temperature and ice core CO_2, respectively. This approach yields slopes $\Delta T_{MAT}/\Delta F_{ice1011}$ of 2.5˚C/(Wm^{-2}) and $\Delta T_{SST}/\Delta F_{ice1011}$ of 1.2˚C/(Wm^{-2}), both with a 2σ regression slope uncertainty ±0.09˚C/(Wm^{-2}) (shown as shading in lower panel of Figure 5). That analysis, however, is not representative of $\Delta T/\Delta F$ of the last 260 kyr (for which we have boron isotope data) because uneven sampling results in almost half of the ice core derived CO_2 data points from the last 20 kyrs, and more than 80% from the last 100kyr. When we repeat the analysis but only include the ice core data that are closest to the ages of the boron isotope record (i.e., 59 samples with ~4 kyr sample interval) we regress $\Delta T_{MAT}/\Delta F_{ice59}$ of 2.5˚C/(Wm^{-2}) and $\Delta T_{SST}/\Delta F_{ice59}$ of 1.3˚C/(Wm^{-2}), both with 2σ regression slope uncertainty of ±0.4˚C/(Wm^{-2}) (Figure 5; MAT and SST regressions shown in red and blue, respectively). We take these ice core CO_2-based numbers to be the "true" answer in our test of the boron isotope-based reconstruction. We note that both $\Delta T_{MAT}/\Delta F_{ice1011}$ and $\Delta T_{MAT}/\Delta F_{ice59}$ are consistent with previous estimates of late Pleistocene ESS climate sensitivity to CO_2 forcing (e.g., see $S_{[CO2]}$ in Table 2 of PALEOSENS, 2012).

In determining the 2σ range of ΔF_{boron} we use the 2σ uncertainties of the boron isotope measurement of every data point conflated with the lowest and highest end-member slope of the ΔpH-to-ΔF relationship (i.e., the slope for $CaCO_3$ and DIC change, respectively; see Figure 2). That is, ΔF_{boron} includes the uncertainty both of the boron isotope

544 measurement as well as the uncertainty of the conversion from ΔpH to ΔF. This treatment makes the assumption that the ΔpH-to-ΔF slope uncertainty is independent between data
546 points, which can be justified because the reconstructed pH change of each sample is caused by a different combination of $CaCO_3$, temperature and DIC change. For the
548 temperature data to be compared with ΔF_{boron} we conflate the uncertainty of the temperature reconstruction (1σ of ±1˚C, as above) with the age uncertainty of the boron
550 isotope data, yielding an effective temperature uncertainty only marginally larger than 1σ of ±1˚C. The regression based on the boron isotope data yields $T_{MAT}/\Delta F_{boron}$ of
552 2.6˚C/(Wm^{-2}) with 2σ regression slope uncertainty of ±0.5˚C/(Wm^{-2}) and $\Delta T_{SST}/\Delta F_{boron}$ of 1.3˚C/(Wm^{-2}) with 2σ of ±0.4˚C/(Wm^{-2}) (shown in black in Figure 5).

554

Direct measurement of CO_2 on air trapped in ice cores yields inherently much more
556 precise and accurate estimates of CO_2 climate forcing than indirect proxy-based approaches, such as the conventional application or our new formalism for the boron
558 isotope system. Our test case illustrates that ice core-based reconstruction of ΔT/ΔF yields more accurate and precise constraints than can be achieved based on boron isotope
560 data, but the difference is rather modest because fractional uncertainty in temperature reconstructions is typically larger than the fractional uncertainty of the CO_2 climate
562 forcing reconstructed based on either ice core or boron isotope data and thus dominates the uncertainty of the regressed slope ΔT/ΔF (i.e., fractional uncertainty referring to the
564 ratio of uncertainty to the overall recorded signal). That is, our test suggests that boron isotope data can in principle be used to reconstruct climate sensitivity with an uncertainty
566 not substantially larger then based on ice core CO_2 data, when the number of data points is the same. More precise constraints on temperature change and more discrete data
568 points are best suited to reduce the uncertainty of the regressed climate sensitivity, rather than further reducing the uncertainty in reconstructed CO_2 climate forcing. We highlight
570 that our formalism yields adequate constraints on climate forcing without requiring any assumption of a second carbonate system parameter, without knowledge of the carbonate
572 chemistry equilibrium constants (i.e., pK_0, pK_1, pK_2; which are strongly dependent on temperature and the major ion composition of seawater), and without highly precise
574 knowledge of the boron isotopic composition of seawater ($\delta^{11}B_{SW}$). Contrary to the

conventional application of the boron isotope system, our formalism yields adequate constraints on climate sensitivity using only the boron isotope data, reconstructed local temperature change (to calculate ΔpK_B for the ΔpH reconstruction, which is a weak function of relative temperature change), and best guess $\delta^{11}B_{SW}$ (see section 3.4; Figure 4), all of which can be obtained from the geologic record significantly older than the reach of ice cores.

4 Discussion and caveats

The boron isotope pH proxy is firmly established as a tool to reconstruct past ocean pH (e.g., Zeebe and Wolf-Gladrow, 2001; Hemming and Hönisch, 2007; Rae et al., 2011; Foster and Rae, 2016) and its usage to place constraints on past ocean acid/base chemistry is rapidly increasing. Furthermore, if the sample material originates from the highly stratified and close to air/sea equilibrated subtropical surface, with auxiliary constraints on ambient temperature and an assumption on a second carbonate system parameter (such as DIC, alkalinity, etc.) the boron isotope pH proxy is routinely extended to reconstruct past atmospheric CO_2 and its radiative forcing of climate change. It is well established (e.g., Pearson and Palmer, 2000; Raitzsch and Hönisch, 2013; Greenop et al., 2017) that this conventional approach relies heavily on accurate and independent knowledge of past seawater boron isotopic composition ($\delta^{11}B_{SW}$) and on the (explicitly or implicitly) assumed seawater carbon content (DIC), alkalinity (ALK), or $CaCO_3$ saturation state. Beyond the last few million years of Earth history both $\delta^{11}B_{SW}$ and these second carbonate system parameters are poorly known, thereby stifling the use of the boron isotope proxy system to investigate the role of the global carbon cycle in forcing climate change throughout most of geologic time. With this paper we hope to lay the groundwork for the robust application of the boron isotope proxy system for geologic periods when $\delta^{11}B_{SW}$, a second carbonate system parameter such as DIC, and/or absolute temperature cannot be determined with the previously required degree of accuracy.

In this study we propose three main new concepts to extend the utility of the boron isotope proxy system, respectively relating to (1) $\delta^{11}B_{SW}$, (2) the need for a second

carbonate system parameter, and (3) the role of temperature change via its effect on carbonate chemistry equilibrium constants and Henry's law.

First, we demonstrate that when $\delta^{11}B_{SW}$ is poorly constrained the boron isotope proxy system can be used to robustly reconstruct ΔpH, but not absolute pH (Fig 3). This result is firmly based in first principle theory. We caution, however, that this approach is only applicable to boron isotope time series that cover no more than a few million years because it assumes that $\delta^{11}B_{SW}$ is constant within the dataset. This timescale is fundamentally set by the ocean residence time of boron, which is canonically assumed to be 10-20 million years (Lemarchand et al., 2002) but may be somewhat shorter (Greenop et al., 2017).

Second, we demonstrate that that CO_2 climate forcing (ΔF) and its causal fractional CO_2 change ($\Delta\log CO_2$) are tightly related to pH change (ΔpH) and fractional change in bicarbonate and DIC (i.e., $\Delta\log HCO_3^-$, ΔlogDIC). We argue that both $\Delta\log HCO_3^-$ and ΔlogDIC must be relatively small on timescales shorter than the oceans residence time of carbon with respect to the geologic CO_2 sources and silicate weathering (very roughly 1 million years), such that ΔpH is the overwhelmingly dominant driver of atmospheric CO_2 change and its climate forcing on orbital timescales. That is, even at times when absolute DIC is unknown we argue it is fair to assume that ΔlogDIC and $\Delta\log HCO_3^-$ are small compared to ΔpH reconstructed from a boron isotope dataset that spans no more than a few orbital cycles, akin to the late Pleistocene ice age CO_2 cycles that we use to validate our formalism. We caution that relaxing the DIC constraint in this way does not apply to events of abrupt carbon addition in secular steady state with carbonate compensation (i.e., the Paleocene-Eocene thermal maximum), in which case ΔlogDIC could significantly contribute to ΔF and relying on ΔpH alone would underestimate ΔF.

Third, while temperature significantly affects both the conventional boron isotope pH proxy and the partitioning of carbon between the atmosphere and seawater we show that it has a surprisingly weak effect on the relationship between the range of boron isotope measurements in a given dataset, the ΔpH reconstructed from this data, and on the

636 climate forcing ΔF inferred from it. To be clear, any information on temperature change will improve reconstructed ΔpH and ΔF because it constrains the presumably small ΔpK
638 terms in equations 2 and 12. To achieve these improvements requires only accurate information on temperature differentials (i.e., temperature information needs to be precise
640 but can be inaccurate) such that accurate information on absolute temperatures is not required. This insight is very convenient even if it is the completely coincidental result of
642 the approximately linear temperature dependence of the pK equilibrium constants (i.e., the exponential temperature dependence of the equilibrium constants K; pK = -logK).
644

Considering the advantages and caveats outlined above, how can our new approach be
646 used to make useful inferences about past CO_2 climate forcing? And, what type of boron isotope sampling strategy is best suited to recover robust reconstructions of CO_2 climate
648 forcing? To illustrate and discuss these questions we apply our formalism to four boron isotope datasets (Figure 6): the orbitally-resolved record of the intensification of northern
650 hemispheric glaciation at the Plio-Pleistocene transition by Martinez-Boti et al. (2015), the record across the Middle Miocene Climatic Optimum (MMCO) by Greenop et al.
652 (2014) that exhibits, but does not fully resolve, orbital-timescale boron isotope changes, and the new highly-resolved late and mid Pleistocene records from ODP Site 999 (Chalk
654 et al., 2017), the former of which we used to validate our formalism.

656 All these records are short relative to the residence time of boron in the ocean, which precludes significant change in $\delta^{11}B_{SW}$ over the duration of each time slice. Thus, we use
658 modern $\delta^{11}B_{SW}$ for the Plio-Pleistocene data (39.61‰; Foster et al., 2010), and a lower $\delta^{11}B_{SW}$ value of 37.82‰ for the mid-Miocene (Foster et al. 2012, Greenop et al., 2014).
660 As we demonstrate here (e.g., Figure 4), using slightly different estimates for low mid-Miocene $\delta^{11}B_{SW}$ (e.g., Lemarchand 2002; Raitzsch and Hönisch, 2013; Greenop et al.,
662 2017) would make no significant difference because pH change reconstruction is much less sensitive to the $\delta^{11}B_{SW}$ value than is the reconstruction of absolute pH. For all
664 datasets we calculate ΔpH relative to the average $\delta^{11}B_{borate}$ and relative to the average reconstructed temperature of the respective dataset, using equation 12 without
666 approximation. Hence, we can plot the data on the same axes of pH change and CO_2

climate forcing, but this axis only applies to changes within each respective dataset and not to changes between them.

The residence time of carbon relative to total weathering is about 200 thousand years but only a fraction of total weathering is due to silicate weathering, such that fractional change of ocean DIC can be assumed to be small on a roughly million-year timescale and shorter. Hence, we cannot quantify a likely small contribution of DIC change (i.e., $\Delta \log HCO_3^-$) to climate forcing e.g., at the onset of the MMCO at 17.2-16.5 Myr or across the duration of the Plio-Pleistocene time slice at 3.3-2.3Myr. However, the orbital-timescale changes evident in all three datasets, as well as the abrupt ~2.8 Myr step-change associated with the intensification of northern hemisphere glaciation, are too rapid to allow for significant DIC change and must therefore satisfy our formalism, as is supported by the good agreement with the ice-core CO_2 data (Figure 3, Figure 6). As a caution, the orbital-timescale fluctuations during the MMCO are not fully resolved, often supported only by single low-$\delta^{11}B$ data points and thus prone to be questioned as being outliers. In this context, using a boron isotope record that is sufficiently resolved to support orbital-timescale $\delta^{11}B_{borate}$ fluctuations with multiple data points is prudent when aiming to reconstruct climate forcing.

Based on these considerations we argue that datasets that fully resolve orbital timescales over the course of time slices not significantly longer than about one million years are most suited for the reconstruction of pH change and CO_2 climate forcing. To the best of our knowledge such datasets are exceedingly rare at the moment, with most efforts currently aimed at generating long-term, low-resolution records that require highly uncertain corrections for $\delta^{11}B_{SW}$ and DIC change to reconstruct CO_2 climate forcing. In the absence of detailed constraints on $\delta^{11}B_{SW}$ and a second carbonate system parameter (e.g., DIC), we argue that only a sampling strategy that targets relatively abrupt transitions or orbital cyclicity can yield robust quantification of pH change and the associated CO_2 climate forcing. Furthermore, samples should be taken from low-latitude open-ocean sites that are close to CO_2 equilibrium with the atmosphere, and exclude time intervals with known biogeochemical aberrations (such as widespread anoxia or euxinia)

698 that may violate our formalism. With these caveats, we demonstrate that boron isotope data can yield adequate constraints on CO_2 climate forcing.

700

Ultimately, we hope the formalism, theory and validation presented in this study opens 702 the door to utilize the boron isotope proxy system to derive quantitative constraints on the various types of climate sensitivity (e.g. equilibrium and Earth system, ECS and ESS 704 respectively; cf. Lunt et al., 2010; PALEOSENS Project Members, 2012). Combined with independent climate reconstructions and ice sheet modeling (e.g., PALEOSENS 706 Project Members, 2012; Köhler et al., 2015; Royer, 2016) these constraints will enable the mapping out of changes in ESS and ECS (e.g., Köhler et al., 2015; von der Heydt et 708 al., 2016) as the planet transitioned from the early Cenozoic greenhouse to the recurring Pleistocene ice ages, improving our understanding of our planet's climate machine as 710 well as honing projections of its future under continued anthropogenic perturbation.

712 **Acknowledgement**

We thank Sarah Greene, an unnamed referee and the Associate Editor for helpful 714 comments and suggestions. This study was supported by UK Natural Environment Research Council grants NE/K00901X/1 to MPH, NE/I006346/1 to GLF, NE/P011381/1 716 to GLF and MPH, and NE/I528626/1 to TC. The Pleistocene boron isotope data can be found at https://doi.pangaea.de/10.1594/PANGAEA.882551.

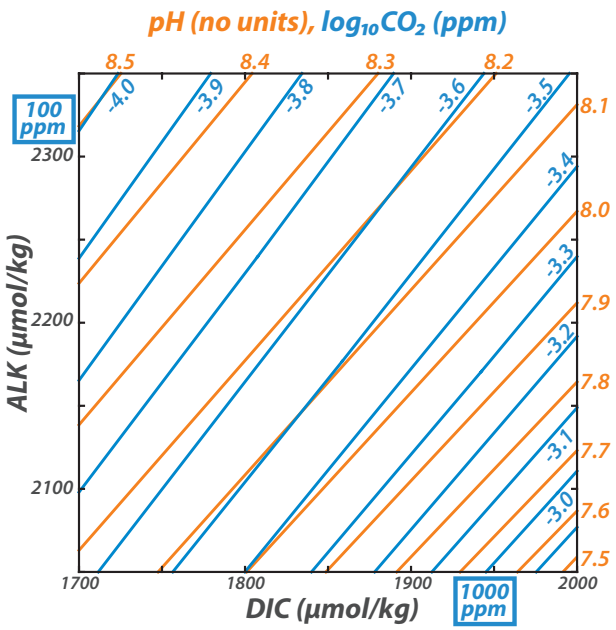

Figure 1. Illustration of the tight coupling between CO_2 and pH. Across a wide range of dissolved inorganic carbon (DIC) and alkalinity (ALK) concentrations contours of constant pH and constant CO_2 are broadly aligned, with similar spacing between pH and $\log_{10}CO_2$ contours. This suggests that H^+ and CO_2 are approximately proportional across the plotted field of DIC and ALK, which covers more than an order of magnitude CO_2 change. In this study we formally explore the mechanisms and implications of the pH-CO_2 relationship in the context of our ability to reconstruct past CO_2 climate forcing.

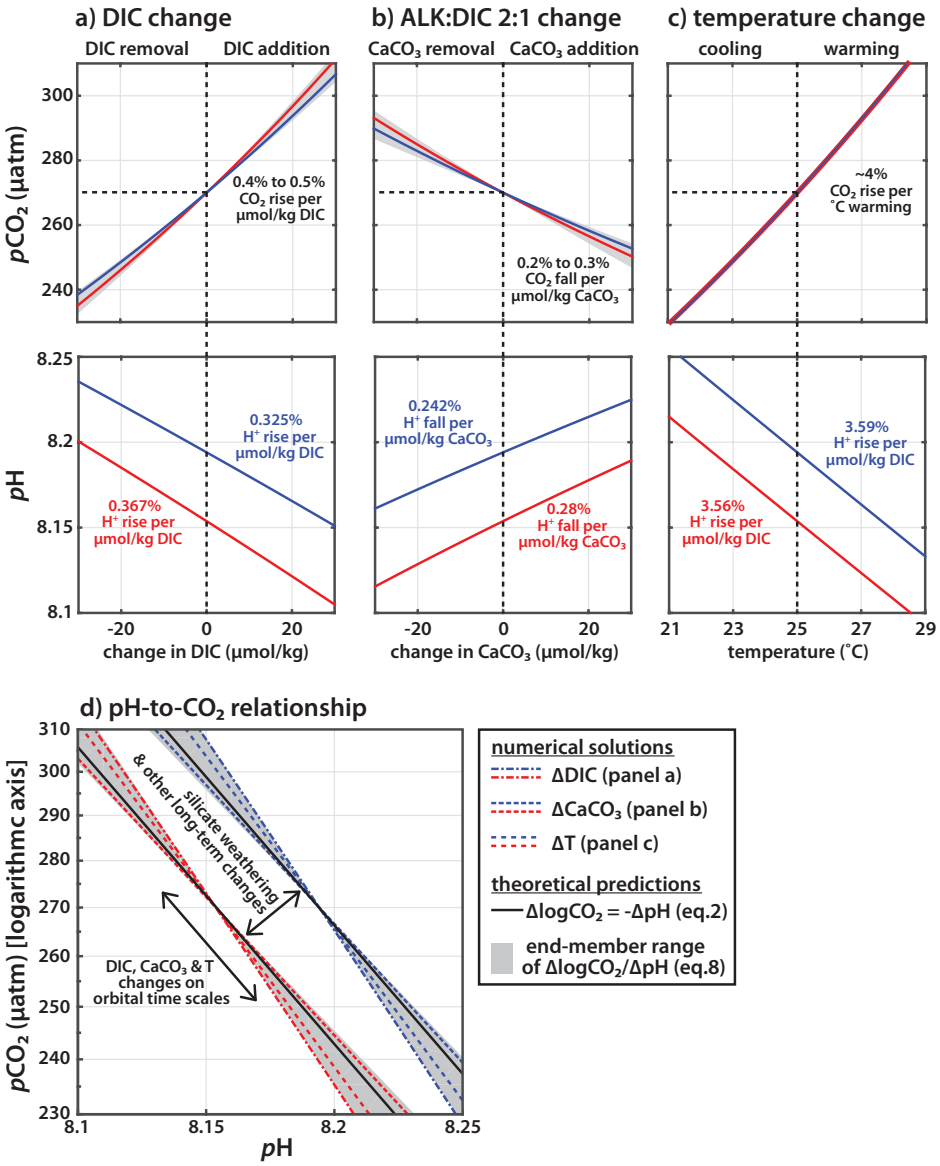

Figure 2. Sensitivity of CO_2 partial pressure and pH to incremental perturbation of (a) DIC, (b) $CaCO_3$ with an alkalinity-to-DIC ratio of 2:1, (c) temperature, and (d) the relationships between CO_2 and pH of experiments (a) to (c). Blue and red lines indicate two separate experiments both with an initial CO_2 of 270 µatm but with initial DIC of 1800 µmol/kg and 2000 µmol/kg, respectively. The black lines in (d) correspond to the pH-CO_2 relationship predicted from equation 2 (solid) and the numerical solutions as shown in panels (a) to (c) (dashed). The purpose of this figure is to demonstrate that fractional changes in CO_2 and H^+ are nearly equal (panels a, b and c), so as to yield ΔpH-to-$\Delta\log_{10}CO_2$ relationships close to -1-to-1 (panel d).

738

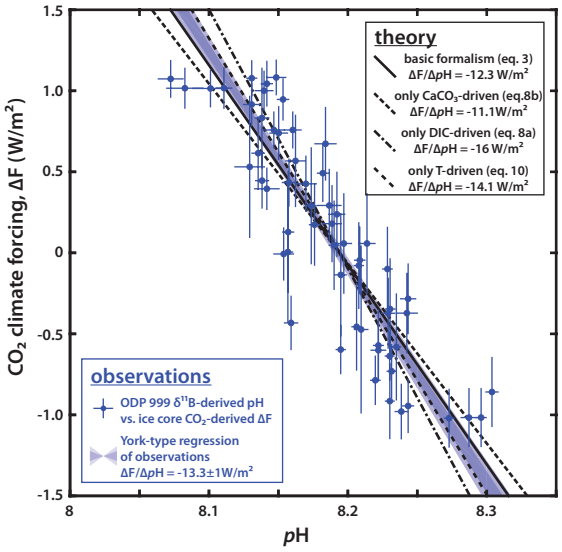

740

Figure 3. Relationship between CO_2 climate forcing from ice-core CO_2 reconstructions
742 and pH from boron isotope record at ODP Site 999. The regression of the data is shown as blue shading, representing the 1σ and 2σ intervals confidence intervals. The regressed
744 slope is statistically indistinguishable from that predicted by theory (equation 3), confirming a ΔpH-to-$\Delta\log_{10}CO_2$ relationship close to -1:1. The fact that the best-fit
746 regressed slope is marginally lower than theory can be taken as evidence for the relative importance in driving glacial/interglacial CO_2 change of whole ocean alkalinity changes
748 via the open system $CaCO_3$ cycle. This result is consistent with consistent with modeling results (Toggweiler, 1999; Hain et al., 2010).

750

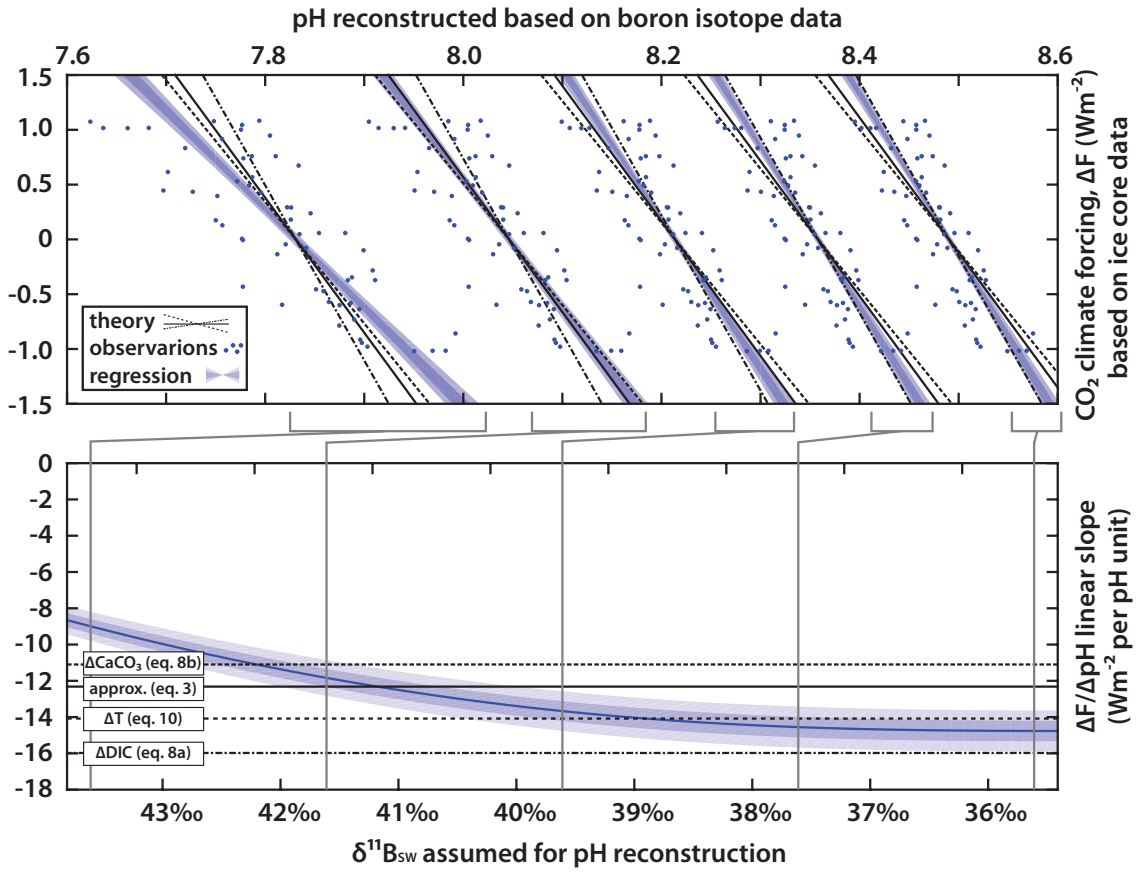

752 **Figure 4.** Relationship between ice core derived CO_2 climate forcing and ODP Site 999 reconstructed pH, as in Figure 3 but this time ignoring reconstructed temperature and 754 systematically introducing error in the seawater boron isotope composition ($\delta^{11}B_{SW}$) assumed in the pH reconstruction. The bottom panel compares observation regressed pH-756 CO_2 slope (blue shading) against theoretical prediction (solid and dashed black lines) as a function of systematically varied $\delta^{11}B_{SW}$. The top panel displays the observed, regressed 758 and predicted pH-CO_2 relationship for five discrete cases: assuming true $\delta^{11}B_{SW}$ as well as deliberately introducing ±2‰ and ±4‰ error in $\delta^{11}B_{SW}$. This exercise demonstrates 760 that reconstructed ΔpH is relatively insensitive to $\delta^{11}B_{SW}$ error, unlike absolute reconstructed pH.

762

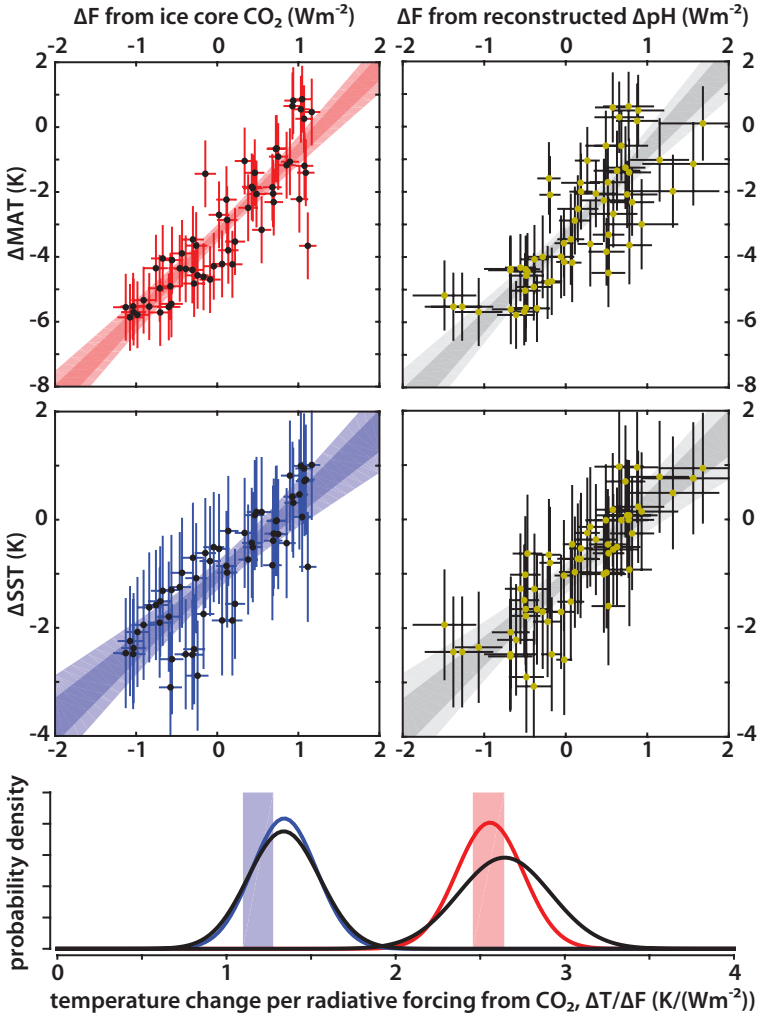

Figure 5. Regression of climate sensitivity ΔT/ΔF based on ice core CO_2 reconstructions (red and blue) and boron isotope data (black/gray), respectively. The four square panels on the top show the regression results using two temperature records, (top) MAT and (bottom) SST (see Martinez-Boti et al., 2015), side by side for the two records of climate forcing (ice core left, and boron isotope right), whereby the ice core data was subsampled to the ages that are closest to the 59 boron isotope data points. The bottom panel shows the probability density functions for the regressed ΔT/ΔF slope from the above panels, compared to the regressed slope for the all ice core CO_2 data of the last 260 kyrs (shading, 2σ). The standard error of ΔF determined from boron isotope data includes measurement uncertainty and the end member range of the ΔpH-to-ΔF conversion.

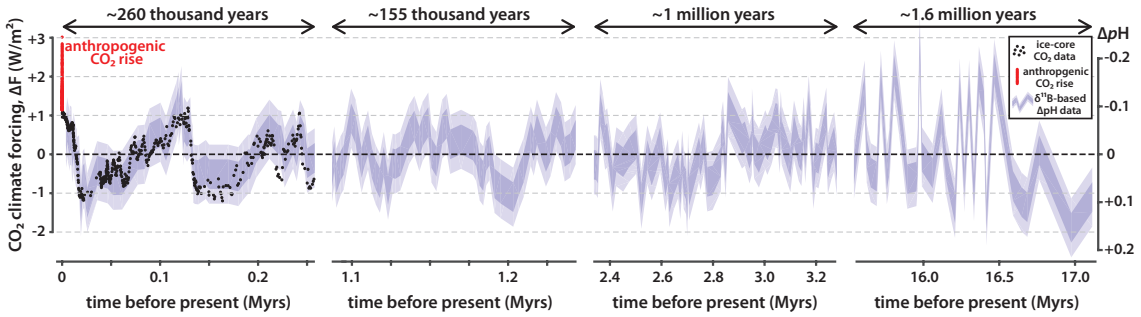

776

Figure 6. Reconstruction of CO_2 climate forcing using equations 3 and 6, based on
778 Pleistocene, Plio-Pleistocene and mid-Miocene boron isotope records of Chalk et al. (2017), Martinez-Boti et al. (2013), and Greenop et al. (2014), respectively, with
780 uncertainty envelope determined empirically from the offset to CO_2 climate forcing calculated from ice core data (black dots). This new approach for reconstructing CO_2
782 climate forcing requires no assumption for a second carbon chemistry parameter and is relatively insensitive to error in $\delta^{11}B_{SW}$. Our formalism quantifies orbital-timescale CO_2
784 climate forcing but not long-term changes such as between the different datasets or trends within the longer Plio-Pleistocene and Miocene datasets. That is, the conversion from
786 ΔpH (right axis) to climate forcing (left axis) according to equation 3 is only valid for records that are shorter than the carbon residence time.

788

References

790 Bereiter, B., S. Eggleston, J. Schmitt, C. Nehrbass-Ahles, T. Stocker, H. Fischer, S. Kipfstuhl, and J. Chappellaz (2015), Revision of the EPICA Dome C CO2 record
792 from 800 to 600kyr before present, *Geophysical Research Letters*, *42*(2), 542-549.

Breecker, D., Z. Sharp, and L. McFadden (2010), Atmospheric CO2 concentrations
794 during ancient greenhouse climates were similar to those predicted for AD 2100, *Proceedings of the National Academy of Sciences of the United States of America*,
796 *107*(2), 576-580.

Broecker, W. S., and T.-H. Peng (1987), The role of CaCO3 compensation in the glacial
798 to interglacial atmospheric CO2 change, *Global Biogeochemical Cycles*, *1*(1), 15-29.

Byrne, B., and C. Goldblatt (2014), Radiative forcing at high concentrations of well-
800 mixed greenhouse gases, *Geophysical Research Letters*, *41*(1), 152-160.

Chalk, T. B., et al. (2017), Causes of ice age intensification across the Mid-Pleistocene
802 Transition, *Proceedings of the National Academy of Sciences of the United States of America*, *114*(50), 13114-13119.

804 Foster, G. (2008), Seawater pH, PCO2 and [CO32-] variations in the Caribbean Sea over the last 130 kyr: A boron isotope and B/Ca study of planktic forminifera, *Earth and*
806 *Planetary Science Letters*, *271*(1-4), 254-266.

Foster, G., P. Pogge von Strandmann, and J. Rae (2010), Boron and magnesium isotopic
808 composition of seawater, *Geochemistry Geophysics Geosystems*, *11*.

Foster, G., C. Lear, and J. Rae (2012), The evolution of pCO(2), ice volume and climate
810 during the middle Miocene, *Earth and Planetary Science Letters*, *341*, 243-254.

Foster, G. L., and J. W. B. Rae (2016), Reconstructing Ocean pH with Boron Isotopes in
812 Foraminifera, *Annual Review of Earth and Planetary Sciences, Vol 44*, *44*, 207-237.

Foster, G., J. Rae, R. Jeanloz, and K. Freeman (2016), Reconstructing Ocean pH with
814 Boron Isotopes in Foraminifera, *Annual Review of Earth and Planetary Sciences, Vol 44*, *44*, 207-237.

816 Foster, G., B. Honisch, G. Paris, G. Dwyer, J. Rae, T. Elliott, J. Gaillardet, N. Hemming, P. Louvat, and A. Vengosh (2013), Interlaboratory comparison of boron isotope
818 analyses of boric acid, seawater and marine CaCO3 by MC-ICPMS and NTIMS, *Chemical Geology*, *358*, 1-14.

820 Franks, P., D. Royer, D. Beerling, P. Van de Water, D. Cantrill, M. Barbour, and J. Berry (2014), New constraints on atmospheric CO2 concentration for the Phanerozoic,
822 *Geophysical Research Letters*, *41*(13), 4685-4694.

Goodwin, P., A. Katavouta, V. M. Roussenov, G. L. Foster, E. J. Rohling, and R. G.
824 Williams (2018), Pathways to 1.5 degrees C and 2 degrees C warming based on observational and geological constraints, *Nature Geoscience*, *11*(2), 102-+.

826 Greenop, R., G. Foster, P. Wilson, and C. Lear (2014), Middle Miocene climate instability associated with high-amplitude CO2 variability, *Paleoceanography*, *29*(9),
828 845-853.

Greenop, R., M. Hain, S. Sosdian, K. Oliver, P. Goodwin, T. Chalk, C. Lear, P. Wilson, and G. Foster (2017), A record of Neogene seawater delta B-11 reconstructed from paired delta B-11 analyses on benthic and planktic foraminifera, *Climate of the Past*, *13*(2), 149-170.

Hain, M., D. Sigman, and G. Haug (2010), Carbon dioxide effects of Antarctic stratification, North Atlantic Intermediate Water formation, and subantarctic nutrient drawdown during the last ice age: Diagnosis and synthesis in a geochemical box model, *Global Biogeochemical Cycles*, *24*.

Hain, M., D. Sigman, J. Higgins, and G. Haug (2015), The effects of secular calcium and magnesium concentration changes on the thermodynamics of seawater acid/base chemistry: Implications for Eocene and Cretaceous ocean carbon chemistry and buffering, *Global Biogeochemical Cycles*, *29*(5), 517-533.

Hain, M. P., D. M. Sigman, and G. H. Haug (2014), The Biological Pump in the Past, *Treatise on Geochemistry* 2nd edition, 485-517.

Hemming, N., and G. Hanson (1992), Boron isotopic composition and concentration in modern marine carbonates, *Geochimica Et Cosmochimica Acta*, *56*(1), 537-543.

Hemming, N. G., and B. Hönisch (2007), Boron Isotopes in Marine Carbonate Sediments and the pH of the Ocean in *Developments in Marine Geology*, pp. 717-734.

Henehan, M., P. Hull, D. Penman, J. Rae, and D. Schmidt (2016), Biogeochemical significance of pelagic ecosystem function: an end-Cretaceous case study, *Philosophical Transactions of the Royal Society B-Biological Sciences*, *371*(1694).

IPCC (2014): Climate Change 2014: Synthesis Report. Contribution of Working Groups I, II and III to the Fifth Assessment Report of the Intergovernmental Panel on Climate Change [Core Writing Team, R.K. Pachauri and L.A. Meyer (eds.)]. *IPCC*, Geneva, Switzerland, 151 pp.

Klochko, K., A. J. Kaufman, W. Yao, R. H. Byrne, and J. A. Tossell (2006), Experimental measurement of boron isotope fractionation in seawater, *Earth and Planetary Science Letters*, *248*(1-2), 276-285.

Knutti, R., and G. C. Hegerl (2008), The equilibrium sensitivity of the Earth's temperature to radiation changes, *Nature Geoscience*, *1*(11), 735-743.

Knutti, R., M. A. A. Rugenstein, and G. C. Hegerl (2017), Beyond equilibrium climate sensitivity, *Nature Geoscience*, *10*(10), 727-+.

Köhler, P., B. de Boer, A. von der Heydt, L. Stap, and R. van de Wal (2015), On the state dependency of the equilibrium climate sensitivity during the last 5 million years, *Climate of the Past*, *11*(12), 1801-1823.

Lemarchand, D., J. Gaillardet, E. Lewin, and C. Allegre (2000), The influence of rivers on marine boron isotopes and implications for reconstructing past ocean pH, *Nature*, *408*(6815), 951-954.

Lemarchand, D., J. Gaillardet, E. Lewin, and C. Allegre (2002), Boron isotope systematics in large rivers: implications for the marine boron budget and paleo-pH reconstruction over the Cenozoic, *Chemical Geology*, *190*(1-4), 123-140.

Lunt, D., A. Haywood, G. Schmidt, U. Salzmann, P. Valdes, and H. Dowsett (2010), Earth system sensitivity inferred from Pliocene modelling and data, *Nature Geoscience*, *3*(1), 60-64.

Martinez-Boti, M., G. Foster, T. Chalk, E. Rohling, P. Sexton, D. Lunt, R. Pancost, M. Badger, and D. Schmidt (2015), Plio-Pleistocene climate sensitivity evaluated using high-resolution CO2 records, *Nature*, *518*(7537), 49-+.

Martinez-Garcia, A., D. Sigman, H. Ren, R. Anderson, M. Straub, D. Hodell, S. Jaccard, T. Eglinton, and G. Haug (2014), Iron Fertilization of the Subantarctic Ocean During the Last Ice Age, *Science*, *343*(6177), 1347-1350.

Myhre, G., E. Highwood, K. Shine, and F. Stordal (1998), New estimates of radiative forcing due to well mixed greenhouse gases, *Geophysical Research Letters*, *25*(14), 2715-2718.

Pagani, M. (2014), Biomarker-Based Inferences of Past Climate: The Alkenone pCO_2 Proxy, *Treatise on Geochemistry* 2nd edition, pp. 361-378.

Pagani, M., D. Lemarchand, A. Spivack, and J. Gaillardet (2005), A critical evaluation of the boron isotope-pH proxy: The accuracy of ancient ocean pH estimates, *Geochimica Et Cosmochimica Acta*, *69*(4), 953-961.

PALEOSENS Project Members (2012), Making sense of palaeoclimate sensitivity, *Nature*, *491*(7426), 683-691.

Pearson, P., and M. Palmer (2000), Atmospheric carbon dioxide concentrations over the past 60 million years, *Nature*, *406*(6797), 695-699.

Rae, J., G. Foster, D. Schmidt, and T. Elliott (2011), Boron isotopes and B/Ca in benthic foraminifera: Proxies for the deep ocean carbonate system, *Earth and Planetary Science Letters*, *302*(3-4), 403-413.

Raitzsch, M., and B. Hönisch (2013), Cenozoic boron isotope variations in benthic foraminifers, *Geology*, *41*(5), 591-594.

Rodenbeck, C., R. Keeling, D. Bakker, N. Metz, A. Olsen, C. Sabine, and M. Heimann (2013), Global surface-ocean p(CO2) and sea-air CO2 flux variability from an observation-driven ocean mixed-layer scheme, *Ocean Science*, *9*(2), 193-216.

Rohling, E. J., G. Marino, G. L. Foster, P. A. Goodwin, A. S. von der Heydt, and P. Koehler (2018), Comparing Climate Sensitivity, Past and Present, *Annual Review of Marine Sciences, Vol 10*, *10*, 261-+.

Royer, D. (2006), CO2-forced climate thresholds during the Phanerozoic, *Geochimica Et Cosmochimica Acta*, *70*(23), 5665-5675.

Royer, D., R. Jeanloz, and K. Freeman (2016), Climate Sensitivity in the Geologic Past, *Annual Review of Earth and Planetary Sciences, Vol 44*, *44*, 277-293.

Shakun, J. D., P. U. Clark, F. He, S. A. Marcott, A. C. Mix, Z. Liu, B. Otto-Bliesner, A. Schmittner, and E. Bard (2012), Global warming preceded by increasing carbon dioxide concentrations during the last deglaciation, *Nature*, *484*(7392), 49-54.

Sigman, D., and E. Boyle (2000), Glacial/interglacial variations in atmospheric carbon

910 dioxide, *Nature*, *407*(6806), 859-869.

Sigman, D., M. Hain, and G. Haug (2010), The polar ocean and glacial cycles in
912 atmospheric CO2 concentration, *Nature*, *466*(7302), 47-55.

Spivack, A., and J. Edmond (1987), Boron isotope exchange between seawater and the
914 oceanic-crust, *Geochimica Et Cosmochimica Acta*, *51*(5), 1033-1043.

Spivack, A., C. You, and H. Smith (1993), Foraminiferal Boron isotope ratios as a proxy
916 for surface ocean pH over the past 21-Myr, *Nature*, *363*(6425), 149-151.

Takahashi, T., et al. (2002), Global sea-air CO2 flux based on climatological surface
918 ocean pCO(2), and seasonal biological and temperature effects, *Deep-Sea Research Part Ii-Topical Studies in Oceanography*, *49*(9-10), 1601-1622.

920 Takahashi, T., et al. (2009), Climatological mean and decadal change in surface ocean pCO(2), and net sea-air CO2 flux over the global oceans, *Deep-Sea Research Part Ii-*
922 *Topical Studies in Oceanography*, *56*(8-10), 554-577.

Vengosh, A., Y. Kolodny, A. Starinsky, A. Chivas, and M. McCulloch (1991),
924 Coprecipitation and isotopic fractionation of Boron in modern biogenic carbonates, *Geochimica Et Cosmochimica Acta*, *55*(10), 2901-2910.

926 van de Wal, R. S. W., B. de Boer, L. J. Lourens, P. Koehler, and R. Bintanja (2011), Reconstruction of a continuous high-resolution CO2 record over the past 20 million
928 years, *Climate of the Past*, *7*(4), 1459-1469.

von der Heydt, A.S., et al. (2016) Lessons on Climate Sensitivity From Past Climate
930 Changes, *Current Climate Change Reports*, 2, 148-158, doi:10.1007/s40641-016-0049-3

932 Wang, X., et al. (2017), Deep-sea coral evidence for lower Southern Ocean surface nitrate concentrations during the last ice age, *Proceedings of the National Academy of*
934 *Sciences of the United States of America*, *114*(13), 3352-3357.

York, D., N. M. Evensen, M. L. Martinez, and J. D. Delgado (2004), Unified equations
936 for the slope, intercept, and standard errors of the best straight line, *American Journal of Physics*, *72*(3), 367-375.

938 Zachos, J. C., G. R. Dickens, and R. E. Zeebe (2008), An early Cenozoic perspective on greenhouse warming and carbon-cycle dynamics, *Nature*, *451*(7176), 279-283.

940 Zeebe, R. E., and D. Wolf-Gladrow (2001), Stable Isotope Fractionation, in *CO2 in Seawater: Equilibrium, Kinetics, Isotopes*, pp. 141-250, Elsevier.